Bioorganic & Medicinal Chemistry Letters 27 (2017) 3744–3748

Contents lists available at ScienceDirect

Bioorganic & Medicinal Chemistry Letters

journal homepage: www.elsevier.com/locate/bmcl

Structure-based optimization and synthesis of antiviral drug Arbidol analogues with significantly improved affinity to influenza hemagglutinin

Zoë V.F. Wright [a], Nicholas C. Wu [b], Rameshwar U. Kadam [b], Ian A. Wilson [b,c,*], Dennis W. Wolan [a,*]

[a] Department of Molecular Medicine, The Scripps Research Institute, La Jolla, CA 92037, USA
[b] Department of Integrative Structural and Computational Biology, The Scripps Research Institute, La Jolla, CA 92037, USA
[c] The Skaggs Institute for Chemical Biology, The Scripps Research Institute, La Jolla, CA 92037, USA

ARTICLE INFO

Article history:
Received 31 May 2017
Revised 24 June 2017
Accepted 27 June 2017
Available online 28 June 2017

Keywords:
Influenza
Hemagglutinin
Arbidol
Structure-based drug design
Bio-layer interferometry

ABSTRACT

Influenza is a highly contagious respiratory viral infection responsible for up to 50,000 deaths per annum in the US alone. The need for new therapeutics with novel modes of action is of paramount importance. We determined the X-ray structure of Arbidol with influenza hemagglutinin and found it was located in a distinct binding pocket. Herein, we report a structure-activity relationship study based on the co-complex combined with bio-layer interferometry to assess the binding of our compounds. Addition of a *meta*-hydroxy group to the thiophenol moiety of Arbidol to replace a structured water molecule in the binding pocket resulted in a dramatic increase in affinity against both H3 (1150-fold) and H1 (98-fold) hemagglutinin subtypes. Our analogues represent novel leads to yield more potent compounds against hemagglutinin that block viral entry.

Influenza annually affects ~5–20% of the US population leading to nearly 200,000 influenza-related hospitalizations per year.[1] While vaccines have produced some measure of control over the risk of infection, rapid antigenic drift makes the selection of which strains to include in the seasonal vaccine an annual challenge. There are currently four licensed influenza drugs available for treatment use in the US; the M2 ion channel inhibitors Amantadine (Symmetrel®) and Rimantadine (Flumadine®),[2] and the neuraminidase (NA) inhibitors Osetlamivir (Tamiflu®) and Zanamivir (Relenza®).[3] However, as resistance to these drugs emerges in current strains, the quest for small molecule therapeutics with novel modes of action becomes more urgent.[4–6]

Arbidol (Umifenovir) is a broad-spectrum antiviral against a number of viruses, including influenza, Ebola, hepatitis B, and hepatitis C.[7,8] Despite initial lack of a known mechanism-of-action against any target virus, Arbidol is clinically used in Russia and China and is currently in phase IV US clinical trials (clinicaltrials.gov/ct2/show/NCT01651663). One major drawback to the use of Arbidol is the large dose required to achieve therapeutic efficacy.[9] Several groups have tried to improve the therapeutic potential by changing the substituents decorating the indole core (Fig. 1A). These have included changes to the nitrogen substituent, the hydroxy group in position 5, the bromo group in position 6, and the thiophenol in position 2.[10–15] However, despite the large number of structure-activity relationship (SAR) studies carried out to date, none of the compounds have shown a vast improvement in binding affinity to both group 1 and group 2 viruses over the parent compound Arbidol. This is perhaps not surprising as the exact binding site was unknown, although the mechanism of action was reported to involve increasing hemagglutinin (HA) stability through preventing the low pH-induced HA transition to the fusogenic state.[9,16,17]

To determine its binding site and mechanism of action, we recently determined crystal structures of Arbidol in complex with the influenza HA viral fusion glycoprotein from the pandemic 1968 H3N2 and recent 2013 H7N9 viruses.[18] Arbidol binds in a conserved hydrophobic cavity at the interface of the HA protomers within the upper stem of the fusion region (Fig. 1B and C). The structures demonstrate the molecular mechanism where Arbidol stabilizes the pre-fusion conformation of HA and prevents the conformational rearrangement required for membrane fusion and subsequent infection.

Using this structural data, we observed that Arbidol binds tightly to the pocket along the edge of the indole core at positions

* Corresponding authors.
E-mail addresses: wilson@scripps.edu (I.A. Wilson), wolan@scripps.edu (D.W. Wolan).

http://dx.doi.org/10.1016/j.bmcl.2017.06.074
0960-894X/

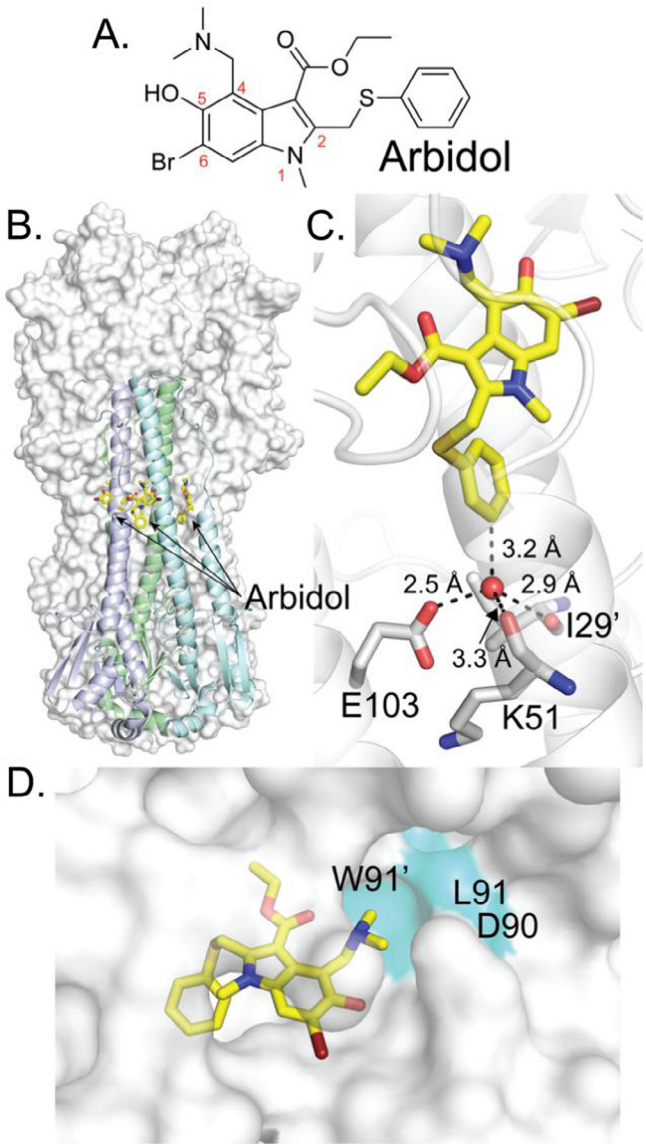

Fig. 1. A. Structure of Arbidol. B. Hemagglutinin trimer (H3 – HK68: A/Hong Kong/1/1968, PDB ID: 5T6N) with the location of the Arbidol binding site within the stem region.[18] C. A highly ordered water molecule adjacent to the Arbidol (yellow carbon, red oxygen, blue nitrogen, mustard sulfur, and maroon bromine) was exploited for structure-based design of Arbidol analogues. D. The HA pocket residues (cyan) near the Arbidol amino group at position 4 that could be used for additional interactions with Arbidol analogues.

1, 5 and 6 (Fig. 1A and C)[10–13] and explains why adding large chemical moieties at these positions can have a deleterious effect on the antiviral efficacy of those molecules.

Our structures also showed that there was additional space within the pocket not fully optimized for binding to the protein by the amino group in position 4 and the thiophenol group at position 2 (Fig. 1A and D). Using our structural data, we designed and synthesized several molecules to exploit these potential additional interactions and thus improve upon Arbidol binding. We herein report a new Arbidol analogue with significantly improved binding to HA in comparison to the parent compound. Our study provides new insights into how to manipulate compounds to bind to the influenza virus and presents exciting evidence for a possible new influenza therapeutic.

Results and discussion

Synthesis of Arbidol analogues

Our co-complex crystal structure of HA with Arbidol showed that there was underutilized space in the binding pocket to accommodate modifications to both the thiophenol group at position 2 and the dimethylamino group at position 4. To investigate the SAR, we optimized the original route to synthesize Arbidol to allow multiple analogues to be made from the common dibrominated intermediate (**2**) (Scheme 1).[19]

Crystallographic data highlighted the importance of a water molecule in the binding pocket in the *meta* position with respect to the thiophenol group. To exploit this potential interaction with HA, we added either an amino or hydroxy group at the *meta* position, as well as extending the size of the ring to investigate the effect of increased conjugation. To investigate the importance of the dimethylamino group, these analogues were synthesized with and without the presence of the amine in position 4 on the indole, as well as replacing the dimethylamino with a piperazine to investigate if any further interactions towards the back of the binding pocket could be beneficial.

The synthesis began with the orthogonal protection and double bromination of the commercially available indole core (**1**) to give **2**, with a yield of 90% over 3 steps. Here the synthesis diverged to provide two separate sets of analogues; in route 1, thiophenol is added to give intermediate **3** in 86% yield. This was followed by reaction with *N,N,N′,N′*-tetramethyldiaminomethane to give Arbidol (**4**) in reasonable yield (51%) (Supplementary Methods). Reaction with two piperazine analogues gave compounds **14** and **15** (77% and 51% respectively). In route 2, various thiols were reacted to give intermediates **8**–**10**.[20,21] These were again reacted with *N,N,N′,N′*-tetramethyldiaminomethane to generate analogues **11**–**13** (Fig. 2).

During the synthesis of compound **11**,[22] it was found that the sulfur was prone to oxidation in the presence of strong acid or base, leading to a range of side products and hindered purification of the final molecule. By decreasing the strength of the base from potassium hydroxide to sodium carbonate in the penultimate step (yield increased to 67%) and changing the solvent from 1,4-dioxane to dichloromethane (increasing the yield to 99%), it was possible to prevent this oxidation from occurring *in situ* during the course of the last two reactions. Further analysis showed that **11** could not be stored in water for long periods of time (>4 h) which meant that biophysical assessments needed to be carried out as soon as the product was dissolved in buffer.

Evaluation of kinetics using bio-layer interferometry

To investigate the binding affinity of the compounds to the HA, the ratio of k_{on} to k_{off} to give K_d was determined by bio-layer interferometry (BLI) using an Octet Red instrument (ForteBio).[23–25] HA was loaded onto streptavidin-coated biosensors (SSA) and incubated with varying concentrations of small molecule in solution. The experiments comprised five steps: (1) baseline acquisition (60 s); (2) HA loading onto sensor (1800 s); (3) second baseline acquisition (120 s); (4) association of small molecule for the measurement of k_{on} (180 s); and (5) dissociation of small molecule for the measurement of k_{off} (180 s).

Arbidol is a broad-spectrum antiviral that can be used to treat influenza infection from both influenza A group 1 and group 2, and influenza B viruses. To test the affinity of our Arbidol analogues, each compound was assessed for binding against one HA from group 1 (H1 – PR8: A/Puerto Rico/8/1934) and one from group 2 (H3 – HK68: A/Hong Kong/1/1968) (Table 1).

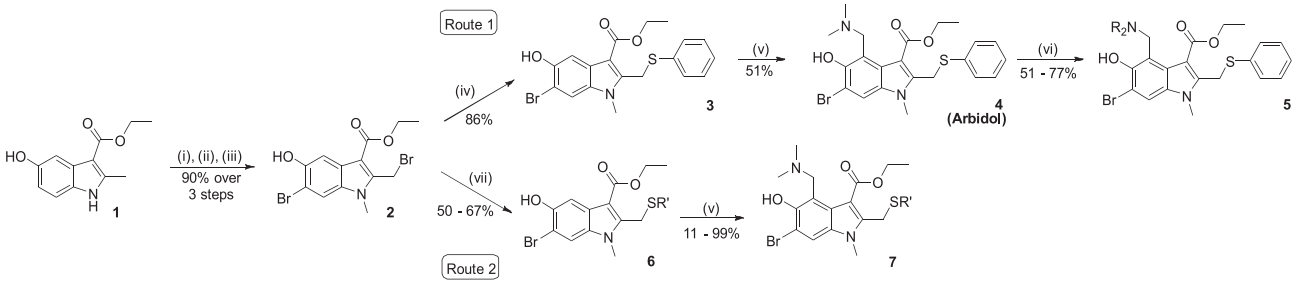

Scheme 1. Synthesis of Arbidol and Analogues. Reagents and conditions: (i) acetic anhydride, pyridine (ii) MeI, NaH, DMF (iii) Br2, CCl4 (iv) thiophenol, KOH, MeOH (v) N,N, N′,N′-tetramethyldiaminomethane, 1,4-dioxane (vi) amine, 1,4-dioxane (vii) R'SH, KOH, MeOH.

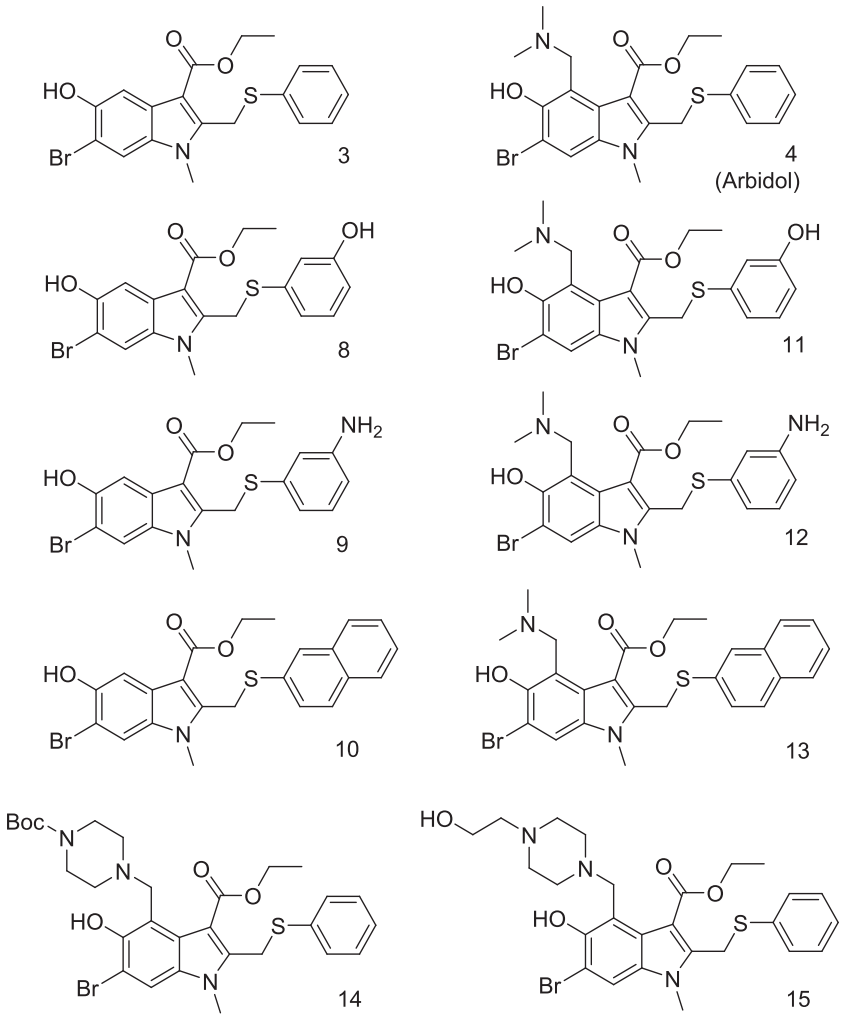

Fig. 2. Analogues of Arbidol.

As with previous Arbidol-based compounds, many of our analogues did not have improved affinity for HA over the parent compound. For example, increasing the size of the group at indole position 4 from a dimethylamino group to a piperazine did not dramatically improve binding to H3 (Table 1, compounds **14** and **15**) and indeed compound **15** did not show any binding to H1. Similarly, increasing the size of the aromatic ring at position 2 (compounds **10** and **13**) did not generate improved interactions, nor did the addition of a *meta*-NH_2 with respect to the thiol (compounds **9** and **12**). Of particular interest was the observation that the binding affinity appeared to improve eightfold when the dimethylamino group at indole position 4 on Arbidol was removed for H3 HA, which was not predicted by the structural data (compounds **3** and **4**).

The most interesting analogue of the SAR set was compound **11** which showed an 98-fold increase in binding with respect to Arbidol against H1 and a 1150-fold increase in binding against H3 (Table 1). This is a marked improvement in the binding affinity observed for compound **12**, presumably due to orbital steering of lone pairs leading to non-optimal hydrogen bonding. It is interesting to note that contrary to compounds **3** and **4**, here removal of the dimethylamino group at position 4 of **11** substantially

Table 1
BLI Measurements of Arbidol Analogues.

Compound	K_d (μM)			
	PR8 (H1)	R^2	HK68 (H3)	R^2
3	38 ± 2	0.92	11 ± 1	0.82
4 (Arbidol)	47 ± 1	0.97	92 ± 13	0.78
8	75 ± 4	0.91	17 ± 1	0.82
9	no binding	n/a	>100	n/a
10	18 ± 6	0.94	45 ± 6	0.73
11	0.48 ± 0.02	0.96	0.080 ± 0.008	0.86
12	No binding	n/a	7.4 ± 0.4	0.89
13	No binding	n/a	No binding	n/a
14	41 ± 2	0.96	No binding	n/a
15	No binding	n/a	46 ± 3	0.93

decreases binding (compound **8**), but still maintains improved binding against H3 HA (fivefold) with respect to **4**, while displaying a twofold decrease in binding against H1 HA (Table 1, Compound **8**). Importantly, compound **11** was stable throughout the duration of the BLI binding studies.

K_d values were calculated from binding curve data from multiple analyte concentrations using a global fit analysis. This method assumes dissociation of the analyte is rapid and complete and the goodness of fit (R^2) demonstrates the compounds adhered well to the fitting analysis (Table 1, Supplemental Figs. 2 and 3). In addition, due to the strong affinity of compound **11** for HA, we performed a local full fitting calculation. With local fitting, it is assumed that compound dissociation is fully reversible and binding isotherms eventually return to baseline. Compound **11** showed an 85-fold increase against H1 HA (550 ± 120 nM) and an 920-fold increase against H3 HA (100 ± 36 nM), with R^2 values of 0.98 and 0.94 respectively (Supplemental Fig. 4). Importantly, K_d values obtained by both fitting methods for compound **11** were in strong agreement that addition of the *meta* hydroxyl tremendously improved binding affinity to both H1 and H3 HA groups.

Evaluation of the structure-based drug design strategy

Our crystallography data predicted that by attaching a hydroxy group in the *meta*-position, it would be possible to increase the binding by displacing an ordered water molecule in the binding pocket next to Arbidol. To evaluate this strategy, we also synthesized *ortho*- and *para*-hydroxy analogues (Supplementary Fig. 1). We predicted that these compounds would have a decrease in binding affinity with respect to the *meta* analogue as they would not properly align the hydroxyl moiety, and thus could not adequately displace the ordered water molecule and/or provide the necessary hydrogen bonds seen in the Arbidol structure (Fig. 1C).[16]

It was also decided to test the affinity of the *meta*-methoxy compound, which has shown promise in the treatment of Hepatitis B.[13] To further investigate the effect of the amine substitution in position 4, analogues were synthesized with and without this moiety. Compound **20** could not be synthesized using the designed route as double addition of the dimethylamino group adding to both the indole and the *para*-hydroxy ring was observed (Supplementary Fig. 1).

The compounds were again tested in the BLI assay, with H1 and H3 representing group 1 and group 2 viruses. As predicted from our co-complex crystal structures, no binding was observed with either the *ortho*- or *para*-hydroxy substituted rings. Replacing the *meta*-hydroxy group with a methoxy substituent also did not exhibit any binding, possibly because the methoxy group is not a hydrogen bond donor and the larger group will cause van der Waals clashes in the binding pocket.

Conclusions

Utilizing structure-based drug design, we have been able to further probe the structure-activity relationship of the binding site of Arbidol on the influenza HA fusion protein. Previous work by other groups has shown that many substitutions to Arbidol do not lead to increased binding affinity of analogues to both group 1 and group 2 viruses.[10,11,13] Comparison of the previous modifications of Arbidol with our recent crystal structure of Arbidol bound to the influenza HA[18] showed that these prior attempts at improvement interfered with key interactions that Arbidol makes within a hydrophobic binding pocket in the HA stem. In particular, substitutions at indole positions 5 and 6 interfere with binding to W92 of helix C and E90′, Y94′ and K310′ of helix C' in the adjacent subunit trimer. Our work aimed to take advantage of our recent crystal structure to design modifications which increased interactions, filled unoccupied pockets in the HA, or displaced a structured water molecule that was bound adjacent to Arbidol, to exploit possible additional interactions which would increase binding of Arbidol analogues. Indeed, replacement of the thiophenol ring with a *meta*-hydroxythiophenol to generate **11**, resulted in impressive 98-fold and 1150-fold increases in affinity against H1 and H3 HAs, respectively. To validate the initial structure-based prediction, we also synthesized *ortho*- and *para*-substituted thiophenols, which had no detectable binding as measured by bio-layer interferometry. The *meta*-methoxy compounds **18** and **21**, which showed promise against Hepatitis B,[13] were also assessed and lacked ability to interact with H1 and H3 HAs. Our highly improved Arbidol analogue clearly illustrates that the replacement of the structured water molecule with a hydrogen bond donor on Arbidol that interacts directly with the HA binding pocket vastly increases binding affinity to H1 and H3 HAs. Our optimized Arbidol represents a new compound with a dramatic increase in affinity.

Currently, the only treatments for influenza involve either inhibiting the M2 ion channel inhibitors[2] or neuraminidase.[3] These mechanisms have already been shown to be prone to resistance in the clinic.[4–6] Arbidol has both a novel mechanism of action and a different binding site to these drugs, as well as a low rate of generation of resistant strains of influenza with respect to adamantane and neuraminidase inhibitors.[14,15] As compound **11** shows a much higher binding affinity in the BLI than Arbidol, it is possible that drugs derived from this initial hit molecule would be far more effective in the treatment of influenza virus. Despite years of over-the-counter use in China and Russia to treat influenza, Arbidol resistance mutations have yet to be reported in the clinic.[9] This lack of alteration thus far to the binding pocket in resistant strains suggests that it might reduce virus viability and that an improved Arbidol analogue would be a critical countermeasure to prevent the spread of both non-pandemic and pandemic disease for years to come.

Our SAR study highlights that an increase in potency can be achieved by displacing a water molecule from inside the binding pocket. Work is ongoing in our laboratory to produce a more stable version of compound **11** that can withstand longer amounts of time in water and increase the potency and selectivity for influenza virus over the parent compound.

Acknowledgments

We thank R. Shenvi and K. Engle for helpful suggestions and M. Elsliger for computational assistance. The authors gratefully acknowledge support from The Scripps Research Institute, the National Institutes of Health R56 AI117675 (to D.W.W. and I.A. W.) and R21 CA181027 (to D.W.W.), Swiss National Science Foundation post-doctoral fellowship (to R.U.K.), and Croucher Foundation Fellowship (to N.C.W.).

A. Supplementary data

Supplementary data associated with this article can be found, in the online version, at http://dx.doi.org/10.1016/j.bmcl.2017.06.074.

References

1. Centers for Disease Control. cdc.gov 2016.
2. Beigel J, Bray M. *Antiviral Res*. 2008;78:91–102.
3. De Clercq E. *Nat Rev Drug Discov*. 2006;5:1015–1025.
4. Bright RA, Shay DK, Shu B, Cox NJ, Klimov AI. *JAMA*. 2006;295:891–894.
5. Moscona A. *N Engl J Med*. 2009;360:953–956.
6. Sheu TG, Fry AM, Garten RJ, et al. *J Infect Dis*. 2011;203:13–17.
7. Pécheur E-I, Borisevich V, Halfmann P, et al. *J Virol*. 2016;90:3086–3092.
8. Blaising J, Polyak SJ, Pécheur E-I. *Antiviral Res*. 2014;107:84–94.
9. Boriskin YS, Leneva IA, Pecheur EI, Polyak SJ. *Curr Med Chem*. 2008;15:997–1005.
10. Brancato V, Peduto A, Wharton S, et al. *Antiviral Res*. 2013;99:125–135.
11. Balzarini J, Ruchko E, Zakharova E, Kameneva I, Nawrozkij M. *Chem Hetero Comp*. 2014;50:489–495.
12. Zotova SA, Korneeva TM, Shvedov VI, et al. *Pharm Chem J*. 1995;29:57–59.
13. Chai H, Zhao Y, Zhao C, Gong P. *Bioorg Med Chem*. 2006;14:911–917.
14. Sellitto G, Faruolo A, de Caprariis P, Altamura S, Paonessa G, Ciliberto G. *Bioorg Med Chem*. 2010;18:6143–6148.
15. Scuotto M, Abdelnabi R, Collarile S, et al. *Bioorg Med Chem*. 2017;25:327–337.
16. Nasser ZH, Swaminathan K, Müller P, Downard KM. *Antiviral Res*. 2013;100:399–406.
17. Leneva IA, Russell RJ, Boriskin YS, Hay AJ. *Antiviral Res*. 2009;81:132–140.
18. Kadam RU, Wilson IA. *Proc Nat Acad Sci USA*. 2017;114:206–214.
19. *General experimental*: Unless otherwise indicated, all reagents were obtained from chemical suppliers with no further purification. Sodium bicarbonate refers to a saturated solution of sodium hydrogen carbonate in water. All water used was either distilled using a Millipore MilliQ® water purifier with Q-Gard® 2 column and 0.22 μM filter from Millipore or used directly from a bottle of HPLC-grade water. All reactions were carried out in closed systems under Argon. NMR spectra were recorded using a Bruker AVIII HD-600, DRX-500, AVIII-400 and DPX-400 spectrometer (600 MHz, 500 MHz, 400 MHz and 400 MHz, respectively) and all samples were dissolved in deuterated chloroform unless otherwise stated. Offline data processing was carried out using the MestreNova software. Chemical shifts (δ) are given in ppm units relative to tetramethylsilane and coupling constants (J) are measured in Hertz. Proton (1H) NMR multiplicities are shown as s (singlet), d (doublet), t (triplet), q (quartet), m (multiplet), dd (double doublet), dt (double triplet), dq (doublet of quartets), dt (doublet of triplets), tt (triplet of triplets), br s (broad singlet), br d (broad doublet). HRMS refers to high resolution mass spectrometry. Electrospray ionization (ESI) accurate mass was determined using a ThermoFinnigan LTQ Ion Trap. Flash column chromatography was carried out using silica gel with particle size ∗60 μm and reverse phase column chromatography was carried out using silica gel 60 silanized (53–200 μm). Thin layer chromatography (TLC) was performed on aluminium backed Sigma-Aldrich TLC plates with F254 fluorescent indicator. Developed plates were air dried and analysed under a UV light or by staining with the appropriate indicator.
20. *Synthesis of Arbidol analogues: Ethyl 5-acetoxy-6-bromo-2-(((3-hydroxyphenyl) thio)methyl)-1-methyl-1H-indole-3-carboxylate* ***8a***: 3-hydroxythiophenol (117 μL, 1.15 mmol, 1.0 eq.) was added to a solution of sodium carbonate (367 mg, 3.46 mmol, 3.0 eq.) and bromo indole **2** (500 mg, 1.15 mmol, 1.0 eq.) in dry ethyl acetate (10 mL). The reaction was heated to 100 °C and stirred for 5 h before cooling, filtering and removing the solvent *in vacuo*. The compound was purified by column chromatography (40% EtOAc in Hexanes) to produce the title product as a pale yellow solid (240 mg, 44%). NMR: δ_H (500 MHz, $CDCl_3$) 7.85 (s, 1H, H_7), 7.56 (s, 1H, H_4), 7.12 (t, J = 7.9 Hz, 1H, H_{13}), 6.95 – 6.90 (m, 1H, H_{14}), 6.78 (s, 1H, H_{10}), 6.75-6.71 (m, 1H, H_{12}), 4.69 (s, 2H, SCH_2), 4.30 (q, J = 7.4 Hz, 3H, $CO_2CH_2CH_3$), 3.66 (s, 3H, NCH_3), 2.40 (s, 3H, $COCH_3$), 1.38 (t, J = 7.4 Hz, 3H, $CO_2CH_2CH_3$). δ_C (150 MHz, $CDCl_3$) 169.8, 165.0, 156.1, 144.6, 143.3, 135.6, 135.1, 130.1, 126.1, 124.8, 119.3, 116.2, 115.3, 113.9, 111.1, 105.8, 60.1, 30.4, 29.9, 21.0, 14.6. R_f: 0.45 (30% EtOAc in Hexane). HRMS (ESI-TOF): $C_{21}H_{20}BrNO_5S$ ($[M+H]^+$) requires 478.0318, found 478.0317.
21. *Synthesis of Arbidol analogues: Ethyl 6-bromo-5-hydroxy-2-(((3-hydroxyphenyl) thio)methyl)-1-methyl-1H-indole-3-carboxylate* ***8***: Sodium carbonate (106 mg, 1.00 mmol, 2.0 eq.) was added to a stirred solution of meta-hydroxy indole **8a** (240 mg, 0.502 mmol, 1.0 eq.) in methanol (40 mL) and left to stir for 2 h. The solution was then filtered and the solvent removed in vacuo. The product was re-dissolved in ethyl acetate (10 mL) and washed once with water (10 mL) before drying (Na2SO4) and concentrating in vacuo to give the title product as a white solid, which could be used without further purification (160 mg, 67%). NMR: δH (600 MHz, MeOD) 7.60 (s, 1H, H7), 7.58 (s, 1H, H4), 7.07 (dd, J = 8.2, 7.7 Hz, 1H, H13), 6.83 - 6.81 (m, 1H, H14), 6.79 (ddd, J = 7.7, 1.8, 0.9, 1H, H10), 6.70 (dd, J = 8.2, 1.8, 0.9 Hz, 1H, H12), 4.70 (s, 2H, SCH2), 4.26 (q, J = 7.1 Hz, 2H, CO2CH2CH3), 3.64 (s, 3H, NCH3), 1.39 (t, J = 7.1 Hz, 3H, CO2CH2CH3). δC (150 MHz, MeOD) 166.9, 158.9, 150.6, 145.5, 136.4, 133.6, 131.0, 130.7, 128.0, 124.9, 120.5, 116.0, 114.8, 107.9, 104.8, 60.8, 30.5, 30.4, 14.8. R_f: 0.45 (1% MeOH in CH2Cl2). HRMS (ESI-TOF): C19H18BrNO4S ([M+H]+) requires 436.0213, found 436.0215.
22. *Synthesis of Arbidol analogues: Ethyl 6-bromo-4-((dimethylamino)methyl)-5-hydroxy-2-(((3-hydroxyphenyl)thio)methyl)-1-methyl-1H-indole-3-carboxylate* ***11***: *Meta*-hydroxy Indole **8** (30.0 mg, 0.069 mmol, 1.0 eq.) and *N,N,N′,N′*-tetramethyldiaminomethane (47.0 μL, 0.344 mmol, 5.0 eq.) were dissolved in CH_2Cl_2 (30 mL). The reaction was heated to reflux for 3.5 h before removing the solvent *in vacuo* to yield the title product as a pale yellow solid (34 mg, 99%). NMR: δ_H (500 MHz, $CDCl_3$) 7.47 (s, 1H, H_7), 7.12 (t, J = 7.9 Hz, 1H, H_{13}), 6.90 (d, J = 7.9 Hz, 1H, H_{14}), 6.90 (d, J = 7.9 Hz, 1H, H_{12}), 6.66 (s, 1H, H_{10}), 4.41 (s, 2H, CH_2NMe_2), 4.34 (s, 2H, CH_2SPh), 4.15 (q, J = 7.1 Hz, 2H, $CO_2CH_2CH_3$), 3.60 (s, 3H, NCH_3), 2.55 (s, 6H, $CH_2N(CH_3)_2$), 1.33 – 1.21 (m, 3H, $CO_2CH_2CH_3$). δ_C (150 MHz, $CDCl_3$) 165.9, 156.7, 150.9, 142.6, 135.1, 132.2, 131.0, 130.0, 128.9, 124.6, 124.3, 119.3, 115.5, 113.4, 108.6, 106.3, 60.8, 58.7, 44.0, 30.4, 29.9, 14.3. R_f: 0.15 (10% MeOH in CH_2Cl_2). HRMS (ESI-TOF): $C_{22}H_{25}BrN_2O_4S$ ($[M+H]^+$) requires 493.0791, found 493.0792.
23. Ekiert DC, Kashyap AK, Steel J, et al. *Nature*. 2012;489:526–532.
24. Wu NC, Xie J, Zheng T, et al. *Cell Host Microbe*. 2017;21:742–748.
25. *Bio-layer interferometry data and analysis*: The K_d for ligand binding to influenza HA was determined by BLI using an Octet Red instrument (ForteBio). Biotinylated HAs, purified as described previously,[23] were used for these measurements. HAs at ∼10–50 μg ml^{-1} in 1× kinetics buffer (PBS, pH 7.4, 2% DMSO and 0.002% Tween 20) were loaded onto streptavidin-coated biosensors and incubated with varying concentrations of small molecule in solution. All binding data were collected at 30 °C. The experiments comprised five steps: (1) baseline acquisition (60 s); (2) HA loading onto sensor (1800 s); (3) second baseline acquisition (120 s); (4) association of small molecule for the measurement of k_{on} (180 s); and (5) dissociation of small molecule for the measurement of k_{off} (180 s). Baseline and dissociation steps were carried out in buffer only. The ratio of k_{on} to k_{off} determines the K_d reported here and is subtracted from a reference well to remove the effects of non-specific binding, as previously described.[24] The R^2 for the model fitting and the standard error of mean (SEM) for the K_d values reported in Table 1 were computed by Octet Data Analysis software version 9.0 (ForteBio).